# Synthesis, Molecular Structure, and EPR Analysis of the Three-Coordinate Ni(I) Complex $[Ni(PPh_3)_3][BF_4]$

**V. V. Saraev,*,† P. B. Kraikivskii,† I. Svoboda,‡ A. S. Kuzakov,† and R. F. Jordan§**

*Irkutsk State University, Str. K. Marksa, 1, Irkutsk, 664003, Russia, Darmstadt University of Technology, Petersenstr. 23, Darmstadt, 64287, Germany, and University of Chicago, 5735 S. Ellis Ave., Chicago, Illinois 60637*

*Received: March 20, 2008; Revised Manuscript Received: September 30, 2008*

The compound $[Ni(PPh_3)_3][BF_4]\cdot BF_3\cdot OEt_2$ was isolated in crystalline form from the olefin oligomerization catalyst system $Ni(PPh_3)_4/BF_3\cdot OEt_2$ and structurally characterized by X-ray diffraction. The influence of vibronic coupling on the EPR parameters of three-coordinate metal complexes with a $3d^9$ electronic configuration was investigated within the framework of ligand field theory. Analytical expressions for **g**-tensor components and isotropic hyperfine coupling constants with ligand nuclei were obtained using first-order perturbation theory. It has been shown that the account of the vibronic interaction in the excited state predicts the existence of three-axial anisotropy of the **g**-tensor even at the level of first-order perturbation theory; two axes of the **g**-tensor located in a plane of three-coordinate structure can rotate about the main *z* axis when a compound is distorted by motion of ligands. It has been shown that in three points of the potential energy surface minimum, for which linear and quadric constants of the vibronic interactions have an identical signs, the HFS isotropic constant from one ligand is larger than HFS constants from the other two; for different vibronic constant signs the ratio between HFS constants varies on opposite. This theoretical researches are in the quality consent with experimental data for a three-coordinate Ni(I) and Cu(II) flat complexes.

## 1. Introduction

The monovalent oxidation state of nickel has received increasing attention in recent years, in part due to its active role in a number of catalytic processes including biochemical reactions,[1] nickel-mediated cross-coupling reactions to make new C−C bonds,[2] alkene oligomerization by heterogeneous[3] and homogeneous nickel catalysts,[4] and other processes.[5] Ni(I) complexes with phosphine ligands are thermally stable and can display high activity in the oligomerization of unsaturated hydrocarbons. For example, in the $Ni(PPh_3)_4/BF_3\cdot OEt_2$ catalyst system, prepared by mixture of the two components in toluene solution, quantitative oxidation of Ni(0) to Ni(I) with formation of cationic Ni(I) phosphine complexes was observed.[4b–d] At a molar ratio of B/Ni = 4/1, the major species formed in this system is the 15-electron, 3-coordinate Ni(I) complex $[Ni(PPh_3)_3][BF_4]$, which displays high activity in styrene oligomerization.[4c]

The characterization of Ni(I) species by EPR is hindered by the lack of a strict theoretical description of EPR spectra for 3-coordinate, homoleptic $d^9$ species. The EPR theory which is advanced well for cubic structures[6] and their derivatives[7] cannot be applied for three-coordinate compounds without corrections as wave functions of a doubly degenerate state in three-coordinate structures are bound by a spin−orbit interaction among themselves.[8]

The influence of covalence on the **g**-tensor and hyperfine interaction with ligands in heteroleptic three-coordinate Cu(II) complexes has been studied in detail,[9] but vibronic interactions were not taken into account. On the other hand, the importance of Jahn−Teller distortions for three-coordinate structures with doubly degenerate electronic states is well appreciated.[10–12]

The trigonal planar three-coordinate complex $[Ni(PPh_3)_3]^+$ has a doubly degenerate ground state, resulting in a Jahn−Teller distortion that reveals itself by three-axial anisotropy of the **g**-tensor ($g_X = 2.07$; $g_Y = 2.12$; $g_Z = 2.38$) and magnetic nonequivalence of the phosphine ligands ($A(1P)_X = 8.1$; $A(1P)_Y = 6.4$; $A(1P)_Z = 6.1$; $A(2P)_{X,Y,Z} < 3$ mT).[13,14] In our previous work,[13] the influence of ground-state vibronic interactions on EPR parameters of three-coordinate $3d^9$-complexes was investigated to aid in interpreting the EPR spectra of $[Ni(PPh_3)_3][BF_4]$ and related complexes. Assuming that the spin−orbital interaction is smaller than the vibronic interaction, analytical expressions that describe the relation between **g**-tensor components ($g_\perp < g_{||}$) were developed using first-order perturbation theory. However, these expressions do not explain existence of three-axial anisotropy of EPR parameters.

In the present work, the complex $[Ni(PPh_3)_3][BF_4]\cdot BF_3\cdot OEt_2$ was obtained in crystalline form from the $Ni(PPh_3)_4/BF_3\cdot OEt_2$ catalyst system and characterized by X-ray diffraction. Additionally, the influence of vibronic interactions on the EPR parameters for three-coordinate $3d^9$ complexes has been investigated in more detail within the framework of the ligand field theory and considering the electron−oscillator interactions both in ground and in excited states. Analytical expressions for **g**-tensor components and isotropic hyperfine coupling constants with ligand nuclei were obtained using first-order perturbation theory. These expressions were used to interpret the EPR spectra of the $[Ni(PPh_3)_3][BF_4]$ and related species.

## 2. Experimental Section

All operations were carried out under argon using Schlenk techniques. Toluene and benzene (Merck) were distilled from

* Corresponding author. E-mail: saraev@admin.isu.ru.
† Irkutsk State University.
‡ Darmstadt University of Technology.
§ University of Chicago.

10.1021/jp802462x CCC: $40.75 
Published on Web 11/08/2008

**TABLE 1: Crystal Data for Complex $[Ni(PPh_3)_3]BF_4 \cdot BF_3 \cdot OEt_2$**

| empirical formula | $C_{58}H_{55}B_2F_7NiOP_3$ |
|---|---|
| formula mass | 1073.29 |
| crystal size | 0.36 × 0.20 × 0.10 |
| crystal system | triclinic |
| space group | $P\bar{1}$ |
| $a$ (Å) | 13.318(1) |
| $b$ (Å) | 13.946(1) |
| $c$ (Å) | 17.017(1) |
| α (deg) | 76.880(9) |
| $\beta$ (deg) | 68.233(9) |
| $\gamma$ (deg) | 83.948(8) |
| $V$ (Å$^3$) | 2857.9(3) |
| $Z$ | 2 |
| $D_{calcd}$ (g/cm$^3$) | 1.387 |
| $\mu$(Mo Kα) (mm$^{-1}$) | 0.491 |
| temperature (K) | 100 |
| data collection range (deg) | $4.09 \geq 2\Theta \geq 26.37$ |
| $H$ | $-16 \geq h \geq 16$ |
| $K$ | $-17 \geq k \geq 17$ |
| $L$ | $-21 \geq l \geq 20$ |
| no. reflections measured | 34892 |
| no. unique data | 11644 [$R$(int) = 0.0878] |
| parameters | |
| GoF on $F^2$ | 1.033 |
| $R1$ [$I \geq 2\sigma(I)$] | 0.0845 |
| $wR2$ (all data) | 0.2042 |

sodium/benzophenone prior to use. $BF_3(OEt_2)$ (Merck) was distilled over LiH before use. $Ni(PPh_3)_4$ was synthesized by a literature method.[15]

Infrared spectra were recorded on a Bruker FRA 106 spectrometer. EPR spectra were recorded on a CMS-8400 instrument (9.6 GHz) at 77 K.

**Crystal Structure Analysis.** Crystal data are listed in Table 1. Data collection: a crystal was sealed under argon in a glass capillary and mounted on an Oxford Excalibur diffractometer. Reflections were measured ($\omega$-scans) using graphite-monochromated Mo Kα radiation; Lp correction and absorption correction based on $\psi$-scans were applied. The structure was solved by direct and conventional Fourier methods. All non-hydrogen atoms were treated with a riding model in idealized positions.

Crystallographic data (excluding structure factors) have been deposited with the Cambridge Crystallographic Data Centre. Copies of the data [CCDC 682428] can be obtained free of charge on application to CCDC, 12 Union Road, Cambridge CB2 1EZ, UK [Fax: (international) + 44(1223)336-033, E-mail: deposit@ccdc.cam.ac.uk].

**$[Ni(PPh_3)_3][BF_4] \cdot BF_3 \cdot OEt_2$.** $BF_3 \cdot OEt_2$ (0.23 mL) was added to a stirred solution of $Ni(PPh_3)_4$ (0.5 g) in toluene (10 mL) over 10 min at 20°. The mixture was cooled to −10 °C, maintained at this temperature for 3 h, and filtered. Pentane (5% by volume) was added to the brown filtrate. The compound $[Ni(PPh_3)_3][BF_4] \cdot BF_3 \cdot OEt_2$ was obtained in 73% yield as yellow crystals from the filtrate by slow crystallization at −20 °C (5−7 days) and filtration at −20 °C. Calcd for $C_{58}H_{55}B_2F_7NiOP_3$ (1073.29): C 64.85, H 5.12, P 8.66. Found: C 65.23, H 4.82, P 8.37. IR (cm$^{-1}$) 3060 w ($\nu$ H−C=), 1580−1980 m ($\nu$ C=C), 1460 s ($\delta_{as}$ PPh), 1440 s ($\delta_{as}$ PPh), 1290 m ($\delta_s$ PPh), 1100−1000 s ($\nu$ $BF_4^-$), 890 vs ($\rho_1$ PPh), 743 m ($\nu$ $BF_4^-$), 690 w ($\rho_1$ PPh), 575 s ($\nu_{as}$ $PC_3$), 520 m ($\nu_s$ $PC_3$). EPR (toluene, 77 K): $g_X = 2.07$; $g_Y = 2.12$; $g_Z = 2.38$; $A(1P)_X = 8.1$; $A(1P)_Y = 6.4$; $A(1P)_Z = 6.1$; $A(2P)_{X,Y,Z} < 3$ mT.

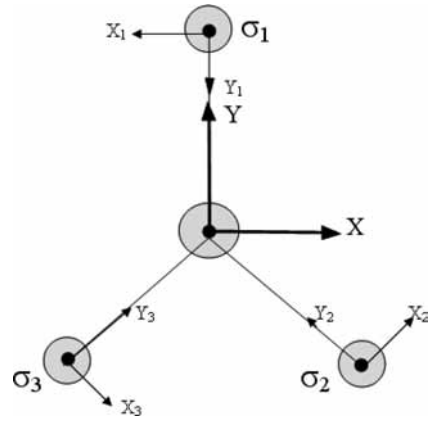


**Figure 1.** Three-coordinate complex of $D_{3h}$ symmetry.

## 3. Theoretical Analysis

Three-coordinate d$^9$-complexes of $D_{3h}$ symmetry (Figure 1) have the ground $E(|x^2 - y^2\rangle, |xy\rangle)$ and excited $E(|yz\rangle, |xz\rangle)$ doubly degenerate states.[8]

Molecular orbitals (MOs) can be represented as linear combinations of metal d-orbitals and corresponding to them by symmetry group orbitals of ligands.[16] In the general form, the MO on which there is unpaired electron is

$$|\Psi\rangle = a|d\rangle - b|\Phi_L\rangle \quad (1)$$

where $|d\rangle$ is d-orbital of the central atom; $|\Phi_L\rangle$ is corresponding by symmetry group orbital of ligands; $a$ and $b$ are coefficients corresponding to the contribution to MO of combining orbitals. Atom orbital (AO) overlapping is not taken into account, and only $\sigma$-orbitals of ligands are considered which consist of s-orbits of atoms from the first coordination sphere.

The ligand group orbitals that combine only with the AOs of a ground orbital doublet have the form:[16]

$$|\Phi_{x^2-y^2}\rangle = \frac{1}{\sqrt{6}}(2\sigma_1 - \sigma_2 - \sigma_3), \quad |\Phi_{xy}\rangle = \frac{1}{\sqrt{2}}(\sigma_2 - \sigma_3) \quad (2)$$

the corresponding MOs can be presented as follows:

$$|\Theta^{(0)}\rangle = a|x^2 - y^2\rangle - b|\Phi_{x^2-y^2}\rangle, \quad |\varepsilon^{(0)}\rangle = a|xy\rangle - b|\Phi_{xy}\rangle,$$
$$|\Theta^{(1)}\rangle = |xz\rangle, \quad |\varepsilon^{(1)}\rangle = |yz\rangle \quad (3)$$

where $|\Theta^{(i)}\rangle$ and $|\varepsilon^{(i)}\rangle$ are symmetrical and asymmetrical MO of orbital doublets, respectively. MO of the excited state includes only d-functions under symmetry conditions.

**Vibronic Interaction.** Doubly degenerate $e$-vibrations are active in Jahn−Teller interactions in three-coordinate d$^9$-complexs having $D_{3h}$ symmetry (Figure 1).[17]

The operator of the vibronic interaction is well-known:[17]

$$\hat{U}^{(i)} = \frac{1}{2}\omega^{(i)2}(Q_\Theta^{(i)2} + Q_\varepsilon^{(i)2})\hat{\sigma}_0 + V^{(i)}(Q_\Theta^{(i)}\hat{\sigma}_z + Q_\varepsilon^{(i)}\hat{\sigma}_x) +$$
$$W^{(i)}[(Q_\Theta^{(i)2} - Q_\varepsilon^{(i)2})\hat{\sigma}_z - 2Q_\Theta^{(i)}Q_\varepsilon^{(i)}\hat{\sigma}_x] \quad (4)$$

where $\hat{\sigma}_j$ are Pauli matrices:

$$\hat{\sigma}_x = \begin{pmatrix} 0 & 1 \\ 1 & 0 \end{pmatrix}, \quad \hat{\sigma}_z = \begin{pmatrix} 1 & 0 \\ 0 & -1 \end{pmatrix}, \quad \hat{\sigma}_0 = \begin{pmatrix} 1 & 0 \\ 0 & 1 \end{pmatrix}$$

$\omega^{(i)}$ is the frequency of $e^{(i)}$-vibrations; $Q_j^{(i)}$ are symmetrized coordinates of $e^{(i)}$-vibrations; $V^{(i)}$ is the constant of a linear vibronic bond; $W^{(i)}$ is the constant of a quadric vibronic bond; $I$ takes on values 0, 1 for the ground and excited states, respectively.

If it is assumed that the vibronic interactions in the ground and excited states are independent of each another, the energies of adiabatic potential surfaces and wave functions corresponding to them can be written as[17]

$$\varepsilon_{\pm}^{(i)}(\rho,\varphi)=\frac{1}{2}\omega^{(i)2}\rho^{(i)2}\pm\varepsilon^{(i)} \quad (5)$$

$$\varepsilon^{(i)}=[V^{(i)2}\rho^{(i)2}+2V^{(i)}W^{(i)}\rho^{(i)3}\cos 3\varphi^{(i)}+W^{(i)2}\rho^{(i)4}]^{1/2} \quad (6)$$

$$|\Psi_{-}^{(i)}\rangle=\cos\Omega^{(i)}|\Theta^{(i)}\rangle-\sin\Omega^{(i)}|\varepsilon^{(i)}\rangle \quad (7)$$

$$|\Psi_{+}^{(i)}\rangle=\sin\Omega^{(i)}|\Theta^{(i)}\rangle+\cos\Omega^{(i)}|\varepsilon^{(i)}\rangle \quad (8)$$

$$\tan 2\Omega^{(i)}=\frac{V^{(i)}\sin\varphi^{(i)}-W^{(i)}\rho^{(i)}\sin 2\varphi^{(i)}}{V^{(i)}\cos\varphi^{(i)}+W^{(i)}\rho^{(i)}\cos 2\varphi^{(i)}} \quad (9)$$

where $\tan\varphi^{(i)}=Q_{\varepsilon}^{(i)}/Q_{\Theta}^{(i)}$, $\rho^{(i)2}=Q_{\Theta}^{(i)2}+Q_{\varepsilon}^{(i)2}$.

Extremes of adiabatic potential surfaces correspond to the points where $\cos\varphi_0^{(i)}=(\pm 1, \mp 1/2)$ The upper sign in this expression complies with the minimum at $V^{(i)}W^{(i)}>0$ ($\varphi_0^{(i)}=0°, 120°, 240°$), the lower one at $V^{(i)}W^{(i)}<0$ ($\varphi_0^{(i)}=60°, 180°, 300°$).[17] In these points, the wave function of the lower adiabatic potential sheet $|\Psi_{-}\rangle$ turns into $|\Theta\rangle$ or $|\varepsilon\rangle$, symmetrical or asymmetrical relative to the plane orthogonal to the distortion direction, respectively.

**Spin−Orbital Interaction.** The operator of the spin−orbital interaction for the central atom has the form[8]

$$H_{\lambda S}=\lambda\mathbf{LS} \quad (10)$$

where $\lambda$ is the spin−orbit coupling constant.

It is necessary to precisely solve the secular equation to allow for this interaction in the ground state in the limits of the vibronic doublet. Wave spin−orbital functions in the zero-order approximation have the following form at that

$$|\pm\rangle_0=\cos\gamma|\Psi_{-}^{\pm(0)}\rangle\pm i\sin\gamma|\Psi_{+}^{\pm(0)}\rangle \quad (11)$$

where $\tan 2\gamma=\varepsilon_\lambda/\varepsilon^{(0)}$ $\varepsilon_\lambda=-a^2\lambda$ is the energy of the spin−orbital interaction in the limits of the lower orbital doublet.

Perturbation theory can be used to take into account the spin−orbit interaction between the ground and excited states. Considering the first-order corrections, let us write the equation

$$|\pm\rangle=|\pm\rangle_0-\frac{1}{2}a^2\lambda(\sin\gamma-\cos\gamma)[\cos(\Omega^{(0)}+\Omega^{(1)})\mp i\sin(\Omega^{(0)}+\Omega^{(1)})]\cdot\left[\frac{i}{\Delta-\varepsilon^{(1)}}|\Psi_{-}^{\mp(1)}\rangle\mp\frac{1}{\Delta+\varepsilon^{(1)}}|\Psi_{+}^{\mp(1)}\rangle\right] \quad (12)$$

where $\Delta$ is the energy gap between the ground and excited orbital doublets.

**Zeeman Interaction.** The effect of magnetic field $\boldsymbol{B}$ on a doubly spin-degenerate ground state $|\pm\rangle$ can be described with the well-known operator for the Zeeman interaction:[6]

$$H_z=\beta_e(\boldsymbol{L}+2\boldsymbol{S})\boldsymbol{B} \quad (13)$$

where $\beta_e$ is the Bohr magneton.

Nonzero components of the effective **g**-tensor of a paramagnetic system are associated with angular mechanical moments by the following relations:[6]

$$\begin{aligned}
g_{zz}&=2\langle+|L_z+2S_z|+\rangle\\
g_{xx}&=\langle-|L_x+2S_x|+\rangle+\langle+|L_x+2S_x|-\rangle\\
g_{xy}&=-i(\langle-|L_x+2S_x|+\rangle-\langle+|L_x+2S_x|-\rangle)\\
g_{yx}&=\langle-|L_y+2S_y|+\rangle+\langle+|L_y+2S_y|-\rangle\\
g_{yy}&=-i(\langle-|L_y+2S_y|+\rangle-\langle+|L_y+2S_y|-\rangle)
\end{aligned} \quad (14)$$

Leaving in matrix elements (14) only members of the zero and first order of smallness, it is possible to obtain the following expressions for **g**-tensor components:

$$g_{zz}=2(1+2a^2\sin 2\gamma) \quad (15)$$

$$g_{yy}=2\cos 2\gamma-\frac{2\lambda a^2}{\Delta^2-\varepsilon^{(1)2}}[\Delta\cos 2\gamma-\varepsilon^{(1)}(\cos\gamma-\sin\gamma)^2\times\cos 2(\Omega^{(0)}+\Omega^{(1)})] \quad (16)$$

$$g_{xx}=2\cos 2\gamma-\frac{2\lambda a^2}{\Delta^2-\varepsilon^{(1)2}}[\Delta\cos 2\gamma+\varepsilon^{(1)}(\cos\gamma-\sin\gamma)^2\times\cos 2(\Omega^{(0)}+\Omega^{(1)})] \quad (17)$$

$$g_{xy}=g_{yx}=\frac{2a^2\lambda\varepsilon^{(1)}}{\Delta^2-\varepsilon^{(1)2}}(\cos\gamma-\sin\gamma)^2\sin 2(\Omega^{(0)}+\Omega^{(1)}) \quad (18)$$

From here it is seen that the consideration of the vibronic interaction in the excited state predicts the existence of three-axial anisotropy of the **g**-tensor even at the level of first-order perturbation theory, the **g**-tensor being of a nondiagonal form ($g_{xy}=g_{yx}\neq 0$) which indicates the variance of **g**-tensor main axes in the plane ($xy$) with molecular axes $x$, $y$. Using standard techniques,[6] it is possible to obtain the main components of the **g**-tensor in the plane ($xy$) and the relation between the molecular coordinate system and the coordinate system in which the **g**-tensor is diagonal:

$$g_{1,2}=2\cos 2\gamma-\frac{2\lambda a^2}{\Delta^2-\varepsilon^{(1)2}}[\Delta\cos 2\gamma\pm\varepsilon^{(1)}(\sin\gamma-\cos\gamma)^2] \quad (19)$$

$$\tan 2\alpha=\frac{2g_{xy}}{g_{yy}-g_{xx}}=\tan 2(\Omega^{(0)}+\Omega^{(1)}) \quad (20)$$

where $\alpha$ is the turning angle of $x$ and $y$ axes in the plane ($xy$).

In expression (19) the functional dependence on $\Omega$ is absent for $g_{1,2}$. It indicates that the main axes of the **g**-tensor 1 and 2 will rotate in coordination about the $z$ axis when a three-coordinate complex is distorted by motion of ligands.

Figure 2 displays the dependence of the **g**-tensor main components on the ratio of energies of the spin−orbit and vibronic interactions ($\varepsilon_\lambda/\varepsilon^{(0)}$). In order to diminish the number of variable parameters, the following simplifications were assumed: (i) energies of the vibronic interaction in the ground and excited states are equal ($\varepsilon^{(0)}=\varepsilon^{(1)}$); (ii) the factor $a$ (the portion of d-orbitals in the ground-state MO) is taken to equal 0.9, which is typical of coordination compounds;[18] (iii) the relation $\varepsilon/\Delta=0.29$ reflects the fact that that under these conditions the difference between $g_1$ and $g_2$ is maximal and satisfies the condition of smallness of the vibronic interaction in comparison with electronic. For example, when $\varepsilon/\Delta=0.10$ the curves for $g_1$ and $g_2$ virtually merge into one line. It is seen from Figure 2 that when the $\varepsilon_\lambda/\varepsilon^{(0)}\rightarrow 0$ components of the **g**-tensor tend to the pure spin value ($g_e=2$). Within the range

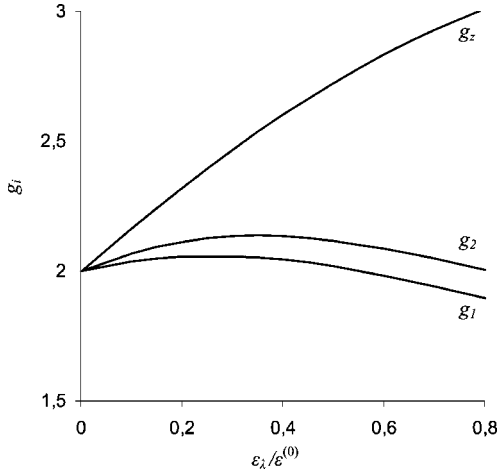


**Figure 2.** Dependence of **g**-tensor components on ratio of energies of spin−orbital and the vibronic interactions ($a = 0.9$; $\Delta/\varepsilon^{(i)} = 3.5$).

$0 < \varepsilon_\lambda/\varepsilon^{(0)} < 0.5$, all components of the **g**-tensor are larger than the pure spin value.

**Hyperfine Interaction (HFI) with Ligand Nucleus.** The Hamiltonian for the contact HFI between electronic and nuclear magnetic moments has the following form[6]

$$H_{SI} = \frac{8\pi}{3} P' \sum_i \delta(r_i) \boldsymbol{I}_i \boldsymbol{S} \tag{21}$$

where $P' = 2g_N\beta_e\beta_N$; $\delta(r_i)$ is the Dirac delta function; $\boldsymbol{I}_i$ is spin of the $i$th nucleus; $\boldsymbol{S}$ is electron spin; $r_i$ is a distance from the $i$th nucleus to electron.

HFS isotropic constants are associated with the contact interaction operator as follows:[6]

$$A_{\mathrm{iso}}^{(i)} = 2P' \left\langle + \left| \frac{8\pi}{3} \delta(r_i) S_z \right| + \right\rangle \tag{22}$$

Isotropic constants for each of the ligands were found using this expression:

$$A_{\mathrm{iso}}^{(1)} = \frac{16\pi}{9} P' b^2 (\cos^2\gamma \cos^2\Omega^{(0)} + \sin^2\gamma \sin^2\Omega^{(0)})$$

$$A_{\mathrm{iso}}^{(2)} = \frac{8\pi}{3} P' b^2 \left[ \frac{1}{6} (\cos^2\gamma \cos^2\Omega^{(0)} + \sin^2\gamma \sin^2\Omega^{(0)}) + \right.$$

$$\left. \frac{1}{2} (\cos^2\gamma \sin^2\Omega^{(0)} + \sin^2\gamma \cos^2\Omega^{(0)}) + \frac{1}{2\sqrt{3}} \cos 2\gamma \sin 2\Omega^{(0)} \right]$$

$$A_{\mathrm{iso}}^{(3)} = \frac{8\pi}{3} P' b^2 \left[ \frac{1}{6} (\cos^2\gamma \cos^2\Omega^{(0)} + \sin^2\gamma \sin^2\Omega^{(0)}) + \right.$$

$$\left. \frac{1}{2} (\cos^2\gamma \sin^2\Omega^{(0)} + \sin^2\gamma \cos^2\Omega^{(0)}) - \frac{1}{2\sqrt{3}} \cos 2\gamma \sin 2\Omega^{(0)} \right] \tag{23}$$

From expressions (23) it follows that $A_{\mathrm{iso}}^{(i)}$ are functions of $\Omega^{(0)}$, and hence, of the angle $\varphi$ (eq 9)).

Figure 3 illustrates angular dependences of the isotropic HFS constants with nuclei of ligands in the linear approximation of the vibronic interaction. From the curves obtained it is seen that in three points of the potential energy surface minimum, $\varphi = 0°$, 120°, 240°, the HFS isotropic constant from one ligand is larger than HFS constants from the other two, and in the points $\varphi = 60°$, 180°, 300°, on the contrary, HFS isotropic constants from two equivalent ligands are larger than from the third ligand. Therefore, if the static Jahn−Teller effect is realized, pairwise magnetic equivalence should be expected. The fact draws attention that in the points of the potential surface minimum both in the first and in the second case constants from

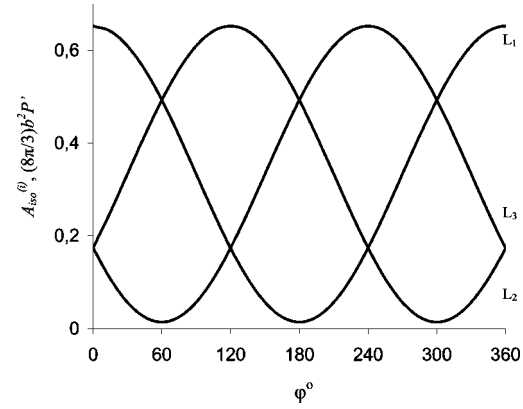


**Figure 3.** Dependence of HFS isotropic constants on the angle $\varphi$ (tan $2\gamma = 0.3$).

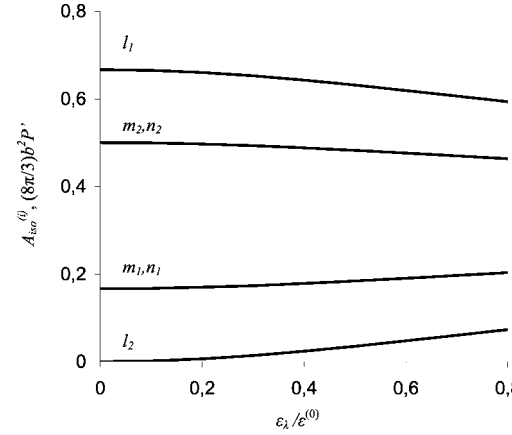


**Figure 4.** Dependence of HFS isotropic constants on the ratio of vibronic and spin−orbital interactions; $l_i$, $m_i$, $n_i$ are numbers of ligands alternately taking on values 1, 2, 3; $i = 1$ under the condition $VW > 0$ ($\varphi = 0°$, 120°, 240°) and $i = 2$ under the condition $VW < 0$ ($\varphi = 60°$, 180°, 300°).

two equivalent ligands remarkably change when the angle $\varphi$ slightly changes, while the constant from the third ligand stays virtually invariant. Hence, one may expect the lines from pairwise equivalent nuclei to broaden in the EPR spectrum.

Figure 4 displays the dependence of HFS isotropic constants on the ratio of energies of the spin−orbital and vibronic interactions in the ground state ($\varepsilon_\lambda/\varepsilon^{(0)}$). It follows from the curves that the more the vibronic interaction prevails over spin−orbital, the larger differences in HFS isotropic constants in potential energy minima. On the other hand, in the extreme case when the spin−orbital interaction prevails over vibronic, ($\varepsilon_\lambda/\varepsilon^{(0)}$) → ∞, all these three constants will equal each other and tend to the value $A_{\mathrm{iso}}^{(i)} = (8\sqrt{2}/9)\pi P' b^2$.

It should be noted that, allowing for the accepted in the present paper hierarchy of the spin−orbital and vibronic interactions, formulas (23) may be used for the description of experimental data only when the vibronic interaction prevails over spin−orbital.

## 4. Results and Discussion

Table 2 contains selected geometrical parameters for $[Ni(PPh_3)_3][BF_4]\cdot BF_3\cdot OEt_2$, and literature data for several similar three-coordinate Ni(0) and Ni(I) phosphine complexes.

As shown in Figure 5, the molecular structure of $[Ni(PPh_3)_3][BF_4]\cdot BF_3\cdot OEt_2$ contains the salt $[Ni(PPh_3)_3][BF_4]$ and 1 equiv of the adduct $BF_3\cdot OEt_2$. The $[Ni(PPh_3)_3]^+$ cation has a flat, approximately T-shaped geometry at Ni (the sum of all

**TABLE 2: Selected Bond Lengths (Å) and Angles (deg) of Molecular Structure for Three-Coordinate Ni(I) and Ni(0) Complexes**

| complex | bond | length (Å) | angle | size (deg) | ref |
|---|---|---|---|---|---|
| $[Ni(PPh_3)_3]BF_4\cdot BF_3\cdot OEt_2$ | Ni1−P1 | 2.215(2) | P1−Ni1−P2 | 107.00(6) | this work |
| | Ni1−P2 | 2.209(2) | P1−Ni1−P3 | 141.98(7) | |
| | Ni1−P3 | 2.183(2) | P2−Ni1−P3 | 110.91(6) | |
| | $Ni-P_{average}$ | 2.202(5) | $\sum(L_i-Ni-L_j)$ | 359.90(9) | |
| | B1−F1 | 1.348(8) | F1−B1−F2 | 106.6(6) | |
| | B1−F3 | 1.359(8) | F1−B1−F3 | 112.3(6) | |
| | B1−F4 | 1.387(8) | F1−B1−F4 | 111.9(6) | |
| | B1−F2 | 1.398(9) | F2−B1−F3 | 106.5(6) | |
| | | | F2−B1−F4 | 107.6(6) | |
| | | | F3−B1−F4 | 111.5(6) | |
| $Ni(PPh_3)_3$[a] | Ni1−P1 | 2.154(2) | P1−Ni1−P2 | 121.2(1) | 19 |
| | Ni1−P2 | 2.148(2) | P1−Ni1−P3 | 118.5(1) | |
| | Ni1−P3 | 2.156(1) | P2−Ni1−P3 | 120.2(1) | |
| | $Ni-P_{average}$ | 2.152(8) | $\sum(L_i-Ni-L_j)$ | 359.9(3) | |
| $Ni(PPh_3)_3$[b] | Ni2−P4 | 2.143(2) | P4−Ni2−P5 | 118.0(1) | 19 |
| | Ni2−P5 | 2.144(2) | P4−Ni2−P6 | 121.7(1) | |
| | Ni2−P6 | 2.139(1) | P5−Ni2−P6 | 120.3(1) | |
| | $Ni-P_{average}$ | 2.142(1) | $\sum(L_i-Ni-L_j)$ | 360.0(3) | |
| $[(Ph_3P)_2NiCl]\bullet THF$ | Ni−P1 | 2.2091(6) | P1−Ni−P2 | 111.52(2) | 25 |
| | Ni−P2 | 2.2012(6) | P1−Ni−Cl | 121.33(2) | |
| | Ni−Cl | 2.1481(6) | P2−Ni−Cl | 126.98(2) | |
| | $Ni-P_{average}$ | 2.2052(1) | $\sum(L_i-Ni-L_j)$ | 359.83(6) | |
| $(Ph_3P)_2NiCl$ | Ni−P1 | 2.2536(5) | P1−Ni−P2 | 114.94(2) | 26 |
| | Ni−P2 | 2.2393(5) | P1−Ni−Cl | 121.12(2) | |
| | Ni−Cl | 2.1666(6) | P2−Ni−Cl | 123.56(2) | |
| | $Ni-P_{average}$ | 2.2465(0) | $\sum(L_i-Ni-L_j)$ | 359.62(6) | |
| $(Ph_3P)_2Ni\{N(SiMe_3)\}_2$ | Ni−P1 | 2.220(4) | P1−Ni−P2 | 107.0(2) | 27 |
| | Ni−P2 | 2.213(4) | P1−Ni−N | 130.4(4) | |
| | Ni−N | 1.88(1) | P2−Ni−N | 122.5(4) | |
| | $Ni-P_{average}$ | 2.216(9) | $\sum(L_i-Ni-L_j)$ | 360.0(0) | |

angles $\sum(P_i-Ni-P_j) = 359.90(9)°$). The largest difference in Ni−P bond lengths is 0.032 Å and that in P−Ni−P bond angles is 34.98(1)°. For comparison, the corresponding largest differences for $Ni(PPh_3)_3$, a diamagnetic Ni(0) complex that exists as two geometrical isomers in a unit cell of single crystal,[19] are 0.007(9) Å and 2.7(0)° for a-isomer and 0.005(1) Å and 3.7(0)° for b-isomer. Apparently, the distortion from trigonal symmetry in $[Ni(PPh_3)_3]^+$ is caused by the Jahn−Teller effect which has static character in the crystal. This conclusion is consistent with ab initio and DFT calculations for $[Au(PH_3)_3]^+$ ($5d^{10}$).[20] Calculations for the singlet ground state ($^1A_1'$) predict a trigonal planar geometry ($D_{3h}$) with the HOMO being the degenerate e′ orbital, which has a predominant $5d_{xy}$, $5d_{x^2-y^2}$ contribution with antibonding Au−P character. Calculations for the lowest triplet excited state ($^3E''$) predict a T-shaped geometry due to a Jahn−Teller distortion.

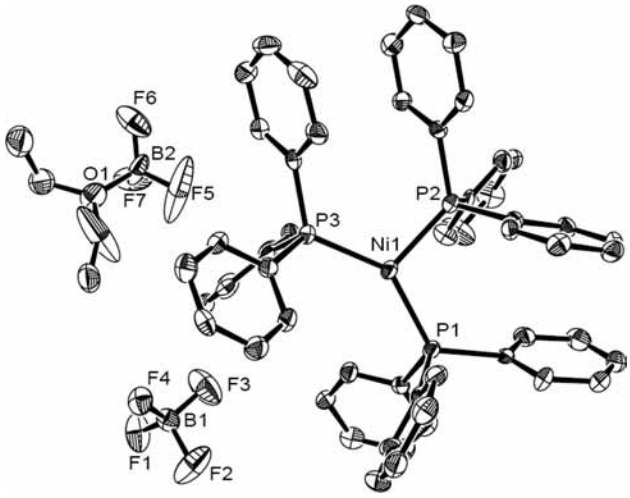


**Figure 5.** Molecular structure of a unit cell for $[Ni(PPh_3)_3]\text{-}BF_4\cdot BF_3\cdot OEt_2$ crystal.

The average Ni−P bond length in $[Ni(PPh_3)_3]^+$ (2.202(5) Å) is slightly greater than that in $Ni(PPh_3)_3$ (2.152(8) and 2.142(1) Å for a-and b-isomers, respectively[19]). A similar trend in metal - phosphorus bond lengths was observed for a large number of phosphine complexes with an electron configurations ranging from $d^1$ to $d^{10}$.[21–24] The M−P bond lengthening upon going to a higher oxidation state is usually ascribed to a reduction in d−$\pi$* backbonding, the $\pi$* orbitals in this case being combinations of the P−C $2e_{x,y}$ MOs and the P 3d orbitals.[21–23]

On the other hand, the average Ni−P bond length in $[Ni(PPh_3)_3]^+$ (2.202(5) Å) is slightly smaller than that in the heteroleptic neutral complexes $[(Ph_3P)_2NiCl]\cdot THF$ (2.2052(1) Å),[25] $(Ph_3P)_2NiCl$ (2.246(1) Å),[26] and $(Ph_3P)_2Ni\{N(SiMe_3)_2\}$ (2.216(9) Å).[27] The average length of the Ni−P bonds in all of complexes listed in Table 2 is less than the Ni−P bond lengths in tetrahedral four-coordinate Ni(I) complexes: $(Ph_3P)_3NiCl$ (2.2979(2) Å);[25] $[(Ph_3P)_3NiCl]\cdot C_7H_8$ (2.3055(5) Å);[28] $(Ph_3P)_3$-NiBr (2.315(6) Å);[29] $[(Ph_3P)_3NiJ]\cdot 0.5THF$ (2.2949(3) Å).[30]

EPR data for homoleptic $d^9$ $[Ni(PR_3)_3]^+$ complexes (R = Ph, Cy), and several heteroleptic Ni(I) and Cu(II) complexes whose structures were established by X-ray diffraction, are listed Table 3. The EPR parameters for $(Ph_3P)_2NiX$ complexes were determined from spectra of these compounds in $(Ph_3P)_2$-$CuX\cdot 0.5C_6H_6$ single crystals;[31] data for the other complexes in Table 3 were determined from spectra of frozen solutions.

According to Table 3, **g**-tensors are rhombic anisotropic for all Ni(I) complexes, and the ratio $g_3 - g_2 > g_2 - g_1$ is generally observed both for homoleptic and the majority of heteroleptic complexes. There is generally good agreement between the experimental values of a **g**-tensor for the considered compounds

**TABLE 3: EPR Data for Selected Three-Coordinate Ni(I) and Cu(II) Complexes**[a]

| complex | $g_1$ | $g_2$ | $g_{3(z)}$ | $A_1$(P), mT | $A_2$(P), mT | $A_{3(z)}$(P), mT | ref |
|---|---|---|---|---|---|---|---|
| $[Ni(PR_3)_3]BF_4$ | | | | | | | |
| R = Ph | 2.07 | 2.12 | 2.38 | 8.1(P1), <3(P2,3) | 6.4(P1), <3(P2,3) | 6.1(P1), <3(P2,3) | 13, 14 |
| R = Cy | 2.10 | 2.17 | 2.40 | 6.4(P2,3), <3(P1) | 6.1(P2,3), <3(P1) | 6.0(P2,3), <3(P1) | 13 |
| $(Ph_3P)_2NiX$ | | | | | | | |
| X = Cl | 2.111 | 2.167 | 2.446 | 6.8(P1), 4.2(P2) | 5.4(P1), 3.8(P2) | 4.8(P1), 3.1(P2) | 31 |
| X = Br | 2.112 | 2.209 | 2.435 | 7.3(P1), 3.5(P2) | 5.1(P1), 3.4(P2) | 4.7(P1), 3.0(P2) | 31 |
| $(N\hat{}N)^{Me}NiL$ | | | | | | | |
| $L = PCy_3$ | 2.03 | 2.17 | 2.54 | | | | 32 |
| L = dppm | 2.03 | 2.16 | 2.43 | | | | 32 |
| L = CO | 2.01 | 2.17 | 2.19 | | | | 33 |
| $(N\hat{}N)^{t\text{-}Bu}Ni(THF)$ | 2.07 | 2.11 | 2.51 | | | | 34 |
| $(N\hat{}N)^{Me}CuX$ | | | | | | | |
| $X = OC_6H_4OMe$ | 2.02 | 2.07 | 2.22 | | | 9.0(Cu) | 35 |
| X = Cl | 2.05 | 2.05 | 2.20 | 0.8(Cu) | 0.8(Cu) | 12.6(Cu) | 36 |
| $X = SCPh_3$ | 2.037 | 2.037 | 2.169 | 0.49(Cu) | 0.97(Cu) | 10.5(Cu) | 9, 36 |
| | | | | 1.0(N) | 1.0(N) | 1.4(N) | |
| $X = SC_6H_3Me_2$ | 2.04 | 2.04 | 2.18 | 1.4(Cu) | 1.4(Cu) | 11.3(Cu) | 9 |

[a] Cy = Cyclohexyl,

dppm = bis(diphenylphosphino)metane,

$(N\hat{}N)^R$ = 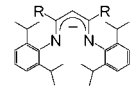

and theoretically designed values of these parameters in a wide range of energy ratio for spin−orbital and Jahn−Teller interactions (Figure 2). One exception is $(N\hat{}N)^{Me}Ni(CO)$, for which the opposite ratio $g_3 - g_2 < g_2 - g_1$ is observed. Apparently, in this case, the influence of the differences in the ligands overrides the effects of the vibronic interaction. A first-order Jahn−Teller effect is not present in $(N\hat{}N)^{Me}Ni(CO)$.[33] $(N\hat{}N)^{Me}CuX$ complexes (X = Cl, $SCPh_3$, $SC_6H_3Me_2$),[9,36] for which $g_3 > g_2 = g_1$, are another exception.

The experimental EPR data for $(Ph_3P)_2NiX$ obtained from $(Ph_3P)_2CuX \cdot 0.5C_6H_6$ single crystal[31] are useful for testing theoretical constructions. It has been shown[31] that the main axis 3($Z$) of the **g**-tensor in a flat $(Ph_3P)_2NiX$ complex is perpendicular to the complex plane and to the main axes $Y_{1-3}$ of the HFS tensors of nonequivalent $^{31}P$ nucleus. The chosen theoretical design (Figure 1) corresponds to the single-crystal EPR data.[31] The magnetic nonequivalence of the $^{31}P$ nuclei in a heteroleptic $(Ph_3P)_2NiX$ complex is coordinated with geometrical nonequivalence of phosphorus atoms and it is the proof of vibronic interactions in heteroleptic complexes too.

Comparing calculated values for the **g**-tensor components (Figure 2) with experimental values for three-coordinate complexes, we come to the conclusion that the calculated values correctly reproduce the experimental data at $\varepsilon_\lambda/\varepsilon^{(0)}$ in the range from 0.05 to 0.5. The experimentally determined HFS constant from $PPh_3$ ligand substantially exceeds those from the other two in homoleptic cationic $[Ni(PPh_3)_3]^+$ complex, indicating the static nature of the Jahn−Teller effect. In compliance with theoretically found values for HFS constants, these points of the minimum are characterized by the identical sign of linear and quadric constants of the vibronic bond ($V^{(i)}W^{(i)} > 0$).

The theoretical expressions derived here can be used to interpret the EPR spectra for other three-coordinate metal complexes with a $3d^9$ electronic configuration. For example, the **g**-tensor for $[Ni(PCy_3)_3][BF_4]$ has rhombic anisotropy also ($g_1 = 2.10$; $g_2 = 2.17$; $g_{3(z)} = 2.40$); however, in this case the HFS constant from the two equivalent $^{31}P$ nucleus is greater than that from the third $^{31}P$ ($A(2P)_1 = 6.4$; $A(2P)_2 = 6.1$; $A(2P)_{3(z)} = 6.0$; $A(1P)_{1,2,3(z)} < 3.0$ mT).[13] Hence, the linear and quadric constants of the vibronic interactions for $[Ni(PCy_3)_3][BF_4]$ have different signs ($V^{(i)}W^{(i)} < 0$).

## 5. Conclusion

The compound $[Ni(PPh_3)_3][BF_4] \cdot BF_3 \cdot OEt_2$ was isolated in crystalline form from the olefin oligomerization catalyst system $Ni(PPh_3)_4/BF_3 \cdot OEt_2$ and structurally characterized by X-ray diffraction. The $[Ni(PPh_3)_3]^+$ cation has a flat T-shaped geometry at Ni. To understand the EPR spectra of $[Ni(PPh_3)_3]^+$ and related three coordinate $d^9$ complexes, the influence of vibronic interactions in both the ground and excited states on the EPR parameters has been investigated within the framework of ligand field theory. Having assumed that spin−orbit interactions are less important than vibronic interactions, analytical expressions for **g**-tensor components and isotropic hyperfine coupling constants with ligand nuclei were obtained using first-order perturbation theory. It has been shown that the account of the vibronic interaction in the excited-state predicts the existence of three-axial anisotropy of the **g**-tensor even at the level of first-order perturbation theory; two axes of the **g**-tensor located in a plane of three-coordinate structure can rotate about the main $z$ axis when a compound is distorted by motion of ligands. It has been shown that, in three points of the potential energy surface minimum, for which linear and quadric constants of the vibronic interactions have an identical signs, the HFS isotropic constant from one ligand is larger than HFS constants from the other two; for different vibronic constant signs the ratio between HFS constants varies on opposite. Results of theoretical researches are in quality equal to experimental data for three-coordinate Ni(I) and Cu(II) flat complexes.

**Acknowledgment.** This work was supported by the RFBR (Russia) and CRDF (USA) (international grant No. RUC1-2862-IR-07). We thank Dr. Ian Steele for assistance with the X-ray crystallographic analysis. P.K. thanks DAAD for a research stipend.

**Supporting Information Available:** Crystal structure report for PK5: $C_{54}H_{45}NiP_3 + C_4H_{10}OBF_3 + BF_4 + C_7H_8$. This material is available free of charge via the Internet at http://pubs.acs.org.

## References and Notes


(1) (a) Medina, M.; Williams, R.; Cammack, R. *J. Chem. Soc., Faraday Trans.* **1994**, *90* (19), 2921–2924. (b) James, T. L.; Cai, L.; Muetterties, M. C.; Holm, R. H. *Inorg. Chem.* **1996**, *35*, 4148–4161. (c) Ge, P.; Riordan, C. G.; Yap, G.-P. A.; Rheingold, A. L. *Inorg. Chem.* **1996**, *35*, 5408–5409. (d) George, S. J.; Seravalli, J.; Ragsdale, S. W. *J. Am. Chem. Soc.* **2005**, *127*, 13500–13501. (e) Piskorski, R.; Jaun, B. *J. Am. Chem. Soc.* **2003**, *125*, 13120–13125. (f) Finazzo, C.; Harmer, J.; Bauer, C.; Jaun, B.; Duin, E. C.; Mahlert, F.; Goenrich, M.; Thauer, R. K.; Doorslaer, S. V.; Schweiger, A. *J. Am. Chem. Soc.* **2003**, *125*, 4988–4989. (g) Duin, E. C.; Cosper, N. J.; Mahlert, F.; Thauer, R. K.; Scott, R. A. *J. Biol. Inorg. Chem.* **2003**, *V. 8* (1−2), 141–148. (h) Gu, W.; Gencic, S.; Cramer, S. P.; Grahame, D. A. *J. Am. Chem. Soc.* **2003**, *125*, 15343–15351. (i) Craft, J. L.; Horng, Y.-C.; Ragsdale, S. W.; Brunold, T. C. *J. Am. Chem. Soc.* **2004**, *126*, 4068–4069. (j) Funk, T.; Gu, W.; Friedrich, S.; Wang, H.; Gencic, S.; Grahame, D. A.; Cramer, S. P. *J. Am. Chem. Soc.* **2004**, *126*, 88–95. (k) Yang, N.; Reiher, M.; Wang, M.; Harmer, J.; Duin, E. C. *J. Am. Chem. Soc.* **2007**, *129*, 11028–11029. (l) Dey, M.; Telser, J.; Kunz, R. C.; Lees, N. S.; Ragsdale, S. W.; Hoffman, B. M. *J. Am. Chem. Soc.* **2007**, *129*, 11030–11032. (m) Kieber-Emmons, M. T.; Riordan, C. G. *Acc. Chem. Res.* **2007**, *40*, 618–625. (n) Harmer, J.; Finazzo, C.; Piskorski, R.; Ebner, S.; Duin, E. C.; Goenrich, M.; Thauer, R. K.; Reiher, M.; Schweiger, A.; Hinderberger, D.; Jaun, B. *J. Am. Chem. Soc.* **2008**, *130*, 10907–10920.

(2) (a) Amatore, C.; Jutand, A. *Organometallics* **1988**, *7*, 2203–2214. (b) Amatore, C.; Jutand, A.; Mottier, L. *J. Electroanal. Chem.* **1991**, *306* (1−2), 125–140. (c) Amatore, C.; Jutand, A. *J. Am. Chem. Soc.* **1991**, *113*, 2819–2825. (d) Courtois, V.; Barhdadi, R.; Troupel, M.; Pe'rrichon, J. *Tetrahedron* **1997**, *53* (34), 11569–11576. (e) Amatore, C.; Jutand, A.; Pe'rrichon, J.; Rollin, Y. *Monatsh. Chem.* **2000**, *131* (12), 1293–1304. (f) Budnikova, Y. H.; Pe'rrichon, J.; Yakhvarov, D. G.; Kargin, Y. M.; Sinyashin, O. G. *J. Organomet. Chem.* **2001**, *630* (2), 185–192. (g) Klein, A.; Budnikova, Y. H.; Sinyashin, O. G. *J. Organomet. Chem.* **2007**, *692* (15), 3156–3166.

(3) (a) Kazansky, V. B.; Elev, I. V.; Shelimov, B. N. *J. Mol. Catal.* **1983**, *21* (1−3), 265–274. (b) Elev, I. V.; Shelimov, B. N.; Kazansky, V. B. *J. Catal.* **1984**, *89* (2), 470–477. (c) Barth, A.; Kirmse, R.; Stach, J. *Z. Chem.* **1984**, *24* (5), 195–196. (d) Cai, F. X.; Lepetit, C.; Kermarec, M.; Oliver, D. *J. Mol. Catal.* **1987**, *43* (1), 93–116. (e) Lepetit, C.; Kermarec, M.; Oliver, D. *J. Mol. Catal.* **1989**, *51* (1), 95–113. (f) Bogus, W.; Kevan, L. *J. Phys. Chem.* **1989**, *93*, 3223–3226. (g) Ghosh, A. K.; Kevan, L. *J. Phys. Chem.* **1990**, *94*, 3117–3221. (h) Bonneviot, L.; Olivier, D.; Che, M. *J. Mol. Catal.* **1983**, *21* (1−3), 415–430. (i) Sohn, J. R.; Shin, D. C. *J. Catal.* **1996**, *160* (2), 314–316. (j) Sohn, J. R.; Park, W. C. *J. Mol. Catal.* **1998**, *133* (3), 297–301. (k) Cai, T. *Catal. Today* **1999**, *51* (1), 153–160. (l) Sohn, J. R. *Catal. Today* **2002**, *73* (1−2), 197–209. (m) Sohn, J. R.; Park, W. C.; Kim, H. W. *J. Catal.* **2002**, *209* (1), 69–74. (n) Sohn, J. R.; Park, W. C. *Appl. Catal. A: Gen.* **2003**, *239* (1−2), 269–278.

(4) (a) Shmidt, F. K.; Saraev, V. V.; Larin, G. M.; Lipovich, V. G. *Izv. Akad. Nauk SSSR, Ser. Khim.* **1974**, *No 1*, 209. (b) Saraev, V. V.; Shmidt, F. K. *Russ. J. Coord. Chem.* **1997**, *23* (1), 40–52. (c) Saraev, V. V.; Kraikivskii, P. B.; Annenkov, V. V.; Vilms, A. I.; Matveev, D. A.; Danilovtseva, E. N.; Ermakova, T. G.; Kuznetsova, N. P.; Lammertsma, K. *Kinet. Catal.* **2005**, *46* (5), 712–718. (d) Saraev, V. V.; Kraikivskii, P. B.; Matveev, D. A.; Vilms, A. I.; Zelinskiy, S. N.; Lammertsma, K. *Kinet. Catal.* **2006**, *47* (5), 699–703. (e) Saraev, V. V.; Kraikivskii, P. B.; Vilms, A. I.; Zelinskii, S. N.; Yunda, A.Yu.; Danilovtseva, E. N.; Kuzakov, A. S. *Kinet. Catal.* **2007**, *48* (6), 778–784. (f) Wang, H. Y.; Meng, X.; Jin, G. X. *Dalton Trans.* **2006**, *7* (21), 2579–2585. (g) Otman, Ya. Ya.; Manulik, O. S.; Flid, V. R. *Kinet. Catal.* **2008**, *49* (4), 479–483.

(5) (a) Dahm, C. E.; Peters, D. G. *J. Electroanal. Chem.* **1996**, *406* (1−2), 119–129. (b) Gennaro, A.; Isse, A. A.; Maran, F. *J. Electroanal. Chem.* **2001**, *507* (1−2), 124–134. (c) Guyon, A. L.; Klein, L. J.; Goken, D. M.; Peters, D. G. *J. Electroanal. Chem.* **2002**, *526* (1−2), 134–138. (d) Ischay, M. A.; Mubarak, M. S.; Peters, D. G. *J. Org. Chem.* **2006**, *71*, 623–628. (e) Esteves, A. P.; Ferreira, E. C.; Medeiros, M. J. *Tetrahedron* **2007**, *63* (14), 3006–3009.

(6) (a) Abragam A.; Bleaney, B. *Electron Paramagnetic Resonance of Transition Ions*; Clarendon Press: Oxford, UK, 1970. (b) Wertz, J. E.; Bolton J. R. *Electron Spin Resonance. Elementary Theory and Practical Applications*; McGraw-Hill Book Co.: New York, 1972. (c) Carrington, A.; McLachlan, A. D. *Introduction to Magnetic Resonance*; Chapman and Hall: London, 1967. (d) Al'tshuler, C. A.; Kozirev B. M. *Electron Paramagnetic Resonance of Intermediate Group Elements*; Science: Moscow, 1972.

(7) (a) McGarvey, B. R. *Can. J. Chem.* **1975**, *53* (16), 2498–2511. (b) Nowlin, T.; Subramanian, S.; Kim, C. *Inorg. Chem.* **1972**, *11*, 2907–2912. (c) Nishida, Y.; Sumita, A.; Kida, S. *Bull. Chem. Soc. Jpn.* **1977**, *50* (9), 2485–2489. (d) Chacko, V. P.; Manoharan, P. T. *J. Magn. Reson.* **1974**, *16* (1), 75–81. (e) Kalbacher, B. J.; Bereman, R. D. *Inorg. Chem.* **1973**, *12*, 2997–3000. (f) Murakami, Y.; Matsuda, Y.; Sakata, K. *Inorg. Chem.* **1971**, *10*, 1734–1738.

(8) Bersuker, I. B. *Electronic Structure and Properties of Coordination Compounds* (in Russian); Khimiya: Leningrad, 1976.

(9) Randall, D. W.; George, S. D.; Holland, P. L.; Hedman, B.; Hodgson, K. O.; Tolman, W. B.; Solomon, E. I. *J. Am. Chem. Soc.* **2000**, *122*, 11632–11648.

(10) Elian, M.; Hoffmann, R. *Inorg. Chem.* **1975**, *14*, 1058–1076.

(11) Komiya, S.; Albright, T. A.; Hoffmann, R.; Kochi, J. K. *J. Am. Chem. Soc.* **1976**, *98*, 7255–7265.

(12) Burdett, J. K. *Inorg. Chem.* **1975**, *14*, 375–382.

(13) Saraev, V. V.; Kraikivskii, P. B.; Lazarev, P. G.; Myagmarsuren, G.; Tkach, V. S.; Schmidt, F. K. *Russ. J. Coord. Chem.* **1996**, *22* (9), 615–621.

(14) Kraikivskii, P. B.; Saraev, V. V.; Matveev, D. A.; Zelinskii, S. N.; Tkach, V. S. *Russ. J. Coord. Chem.* **2003**, *29* (6), 431–434.

(15) Creaves, E. O.; Lock, C. J. L.; Mailtlis, P. M. *Can. J. Chem.* **1968**, *46* (24), 3879–3891.

(16) Dyatkina, M. E. *Basics of the Molecular Orbital Theory* (in Russian); Nauka: Moscow, 1975.

(17) Bersuker, I. B.; Polinger, V. Z. *The vibronic interactions in Molecules and Crystals* (in Russian); Nauka: Moscow, 1983.

(18) Kuska, H. A.; Rogers, M. T. *Electron Spin Resonance of First Row Transition Metal Complex Ions*; Interscience: New York, 1968.

(19) Dick, D. G.; Stephan, D. W.; Campana, C. F. *Can. J. Chem.* **1990**, *68*, 628–632.

(20) Barakat, K. A.; Cundari, T. R.; Omary, M. A. *J. Am. Chem. Soc.* **2003**, *125*, 14228–14229.

(21) Orpen, A. G.; Connelly, N. G. *J. Chem. Soc., Chem. Commun.* **1985**, 1310–1311.

(22) Orpen, A. G.; Connelly, N. G. *Organometallics* **1990**, *9*, 1206–1210.

(23) Davies, M. S.; Aroney, M. J.; Buys, I. E.; Hambley, T. W.; Calvert, J. L. *Inorg. Chem.* **1995**, *34*, 330–336.

(24) Berning, D. E.; Noll, B. C.; DuBois, D. L. *J. Am. Chem. Soc.* **1999**, *121*, 11432–11447.

(25) Ellis, D. D.; Spek, A. L. *Acta Crystallogr. I* **2000**, *56* (9), 1067–1070.

(26) Norman, N. C.; Orpen, A. G.; Quayle, M. J.; Whittell, G. R. *Acta Crystallogr. I* **2002**, *58* (3), m160–m161.

(27) Bradley, D. C.; Hursthouse, M. B.; Smallwood, R. J.; Welch, A. J. *J. Chem. Soc., Chem. Commun.* **1972**, 872–873.

(28) Cassidy, J. M.; Whitmire, K. H. *Acta Crystallogr. I* **1991**, *47*, 2094–2098.

(29) Mealli, C.; Dapporto, P.; Sriyunyongwat, V.; Albright, T. A. *Acta Crystallogr. I* **1983**, *39*, 995–996.

(30) Eckert, N. A.; Riordan, C. G.; Yap, G. P. A. *Acta Crystallogr. (E)* **2006**, *62*, m1766–m1767.

(31) Nilges, M. J.; Barefield, E. K.; Belford, R. L.; Davis, P. H. *J. Am. Chem. Soc.* **1977**, *99*, 755–760.

(32) Bai, G.; Wei, P.; Stephan, D. W. *Organometallics* **2005**, *24*, 5901–5908.

(33) Eckert, N. A.; Dinescu, A.; Cundari, T. R.; Holland, P. L. *Inorg. Chem.* **2005**, *44*, 7702–7704.

(34) Holland, P. L.; Cundari, T. R.; Perez, L. L.; Eckert, N. A.; Lachicotte, R. J. *J. Am. Chem. Soc.* **2002**, *124*, 14416–14424.

(35) Jazdzewski, B. A.; Holland, P. L.; Pink, M.; Young, V. G.; Spencer, D. J. E.; Tolman, W. B. *Inorg. Chem.* **2001**, *40*, 6097–6107.

(36) Holland, P. L.; Tolman, W. B. *J. Am. Chem. Soc.* **1999**, *121*, 7270–7271.


JP802462X